Smithsonian Astrophysical Observatory

RESET

Chandra General Observing Program Performance Report

FormCRG-99-1

1. TYPE OF REPORT: INTERIM [X] FINAL [ ]

[ ] **CHECK HERE IF YOU ARE SUBMITTING THIS REPORT FOR ALL INVESTIGATORS ASSOCIATED WITH THIS PROJECT AND PROVIDE A SUMMARY OF THE EFFORTS OF EACH INDIVIDUAL.**

5. SAO AWARD NUMBER:
GO0-1022X

6. CXC PROGRAM OFFICE APPROVAL & DATE:
For internal use only.

2. NAME & ADDRESS OF THE AWARDEE INSTITUTION:
UW-Madison
Space Science & Engineering Center
1225 W. Dayton, Madison, WI 53706

7. TITLE OF THE PROJECT:
Diffuse X-ray Emission from Nearby Spiral Glaxies

3. NAME OF THE INVESTIGATOR:
Wilton T. Sanders, III

8. PERIOD OF PERFORMANCE:
2/1/2000 - 2/1/2001

4. EQUIPMENT TO REPORT. [If yes, attach Form CE-99-1.]
YES [ ] or NO [X]

9. PATENTS/INVENTIONS TO REPORT. [If yes, attach DD Form 882.]
YES [ ] or NO [X]

10. Explain the objectives of the research and the results obtained, including the Education and Public Outreach [E/PO] component of the Award, if applicable. Please do not exceed 3 pages in length, excluding copies of publications, preprints and related materials.

Please see attached.

11. Cite the title[s] and date[s], or anticipated date[s], of the publication of results:

Please see attached.

12. SIGNATURE OF THE INVESTIGATOR: Wilton T. Sanders

DATE: 3/26/2001

SUBCONTRACTS AND PROCUREMENT DEPARTMENT
GRANT AWARDS SECTION, MAIL STOP 22
1999-2000

Chandra General Observing Program Performance Report
GO0-1022X
Wilton T. Sanders, III

10. Our primary goal is to characterize the spatial distribution and spectral characteristics of the hot interstellar plasma in spiral galaxies. Since it is difficult to see soft X-rays coming from distances greater than a hundred parsec from the Sun in the disk of our Galaxy, we have observed the hot interstellar plasma in a nearby face-on spiral galaxy, NGC 3184. The hot phase of the interstellar medium of normal spiral galaxies is not well characterized or understood, but if the local filling fraction is representative of the Galactic value, its role is fundamental in the evolution of the interstellar medium. Our secondary goal is to constrain the cosmological extragalactic diffuse background below 0.5 keV by quantifying its absorption by this intervening galaxy. Our results so far are described by the two poster papers, which are attached to this report, that we presented at the November 2000 HEAD meeting.

The Juda et al. paper presents the results of a search for X-ray emission in NGC 3184 coming from regions analogous to the Local Bubble. The bubbles that we see in the Milky Way galaxy have typical diameters of 100 pc; at the distance of NGC 3184, they would subtend an angle of ~2.5 arcsec or about 5 pixels in ACIS. Over most of the NGC 3184 field that we searched for sources, the size of the PSF is expected to be < 1 pixel, so we should have no problem resolving bubbles of this size. However, we found no significant evidence that any of the 40 sources detected in the two independent observations of NGC 3184 have extent beyond that of a point source. Thus, our source detections provide no obvious bubble candidates.

But this failure could be due to their faint surface brightness relative to the more diffuse extended emission in the inages, and/or other background. When the backgrounds at energies below 1 keV and are smoothed with an 8-pixel gaussian, both observations show evidence for enhanced emission at the galactic center as well as for enhanced emission coincident with a bright optical feature south-west of the center. While we do not have a "smoking gun" for a superbubble detection, the association of bright peaks in the background maps with the galactic center and a region of enhanced optical emission are suggestive of blow-out regions supplying hot gas to the galactic halo.

The Sanders et al. paper starts with the Juda et al. observation that NGC 3184 shows extended diffuse emission, presumably from the galactic halo. Events were selected from within a circle of diameter 13.5 kpc, centered on the galaxy but excluding the point sources. Background events were taken from the S3 period B data set, an observation of blank sky diffuse background with ROSAT broad band count rates similar to those of the NGC 3184 sky, aligned in RA, Dec, and roll angle to the NGC 3184 observation. Source and background pulse-height distributions were generated in 58-eV-wide bins for each node of the S3 CCD, and CIAO tools were used to create response matrix files and ancillary response files for each node. XSPEC was used to simultaneously fit the four

background-subtracted nodal pulse-height distributions over the 0.3 - 2.2 keV energy range.

We found a semi-acceptable fit, $\chi^2 = 160$ for 132 degrees of freedom, for a model consisting of a MeKaL thermal equilibrium plasma plus a power law. The MeKaL spectrum temperature is kT = 0.2 keV (2.3×10^6 K), and the emission measure is 0.0037 cm^{-6} pc, similar to that of our Galaxy. This thermal component is ~ 20% of the unresolved emission from NGC 3184, and at a distance of 8.1 Mpc, its luminosity is ~ 2×10^{38} erg s^{-1}. We tentatively identify the thermal component with diffuse halo emission from NGC 3184. The luminosity of the power law is 10^{38} erg s^{-1} and we tentatively identify it with emission from unresolved low mass X-ray binaries in NGC 3184. We have not yet searched for spectral differences as a function of position on the face of the galaxy. Better tools for working with extended diffuse emission would be helpful, especially tools for background determination.

The EPO effort has only gotten underway in earnest in the past few months. We are working with the local high school physics teacher to develop a one-semester course in Astrophysics to be taught to upper level students second semester next year. So far, we have been working out the contents and gathering materials.

11. Paper to be submitted to the Astrophysical Journal in 2001.

CXO Observation of Diffuse X-ray Emission from NGC 3184

W. T. Sanders (University of Wisconsin-Madison),
W. Cui (Purdue University),
M. Juda (Smithsonian Astrophysical Observatory),
& D. McCammon (University of Wisconsin-Madison)

ABSTRACT

The low energy diffuse X-ray background that we see in all directions provides evidence for a million-degree phase of the interstellar medium, but its spatial distribution and filling factor are unknown. We have observed NGC 3184, a galaxy that is similar to the Milky Way, with the CXO ACIS to characterize the hot diffuse emission of that galaxy, and to infer the possible distribution of hot gas within our own galaxy. An image of the X-ray emission at energies below 1 keV shows enhanced surface brightness coincident with the galactic spiral arms, probably arising from the halo of NGC 3184, but large hot bubbles or localized regions of diffuse emission are not apparent. The spatial structure and spectral characteristics of the putative halo emission will be presented. This work was funded in part by NASA grants NAG5-3524 and NAG5-629 and SAO grant GO-1022X.

1. INTRODUCTION

- The diffuse X-ray emission of our Milky Way galaxy appears to originate in several different components:
  (1) a number of patchy localized bubbles of one million degree hot gas in the galactic disk, with size scale ~ 100 pc, such as the Local Bubble, the Sco-Cen bubble, the Monogem bubble, and the Orion-Eridanus bubble,
  (2) a number of patchy localized emission regions of one million degree hot gas in the low galactic halo,
  (3) a smooth kpc-scale several-million-degree emission region associated with the Galactic Bulge, and
  (4) smooth ten-kpc-scale several-million-degree emission associated with the high galactic halo.

- Since we are located within the disk of the Galaxy, it is difficult to assess the spatial distributions and filling factors of these components.

- A way to understand more about the hot interstellar plasma in our Galaxy is to study the diffuse emission from other nearly galaxies.

- Such galaxies should be at high galactic latitude to minimize the X-ray absorption by galactic gas, and near to face on to minimize X-ray absorption by the gas of the target galaxy.

- ROSAT observations (Snowden & Pietsch 1995, Cui et al. 1996) detected soft diffuse emission but were unable to eliminate the point source emission from the diffuse emission.

- CXO has the resolution to identify and eliminate point sources having $L_x > 5 \times 10^{36}$ ergs $^{-1}$ in NGC 3184, and NGC 3184 is a suitable target because it is a late type face-on spiral, ~ 8' diameter, with low galactic N_H, 1.15×10^{20} cm^{-2}.

4. SPECTRAL FITS

- XSPEC was used to simultaneously fit the four background-subtracted nodal pulse height distributions over the 0.3 – 2.2 keV energy range.

- Our initial trial spectrum was a MeKaL thermal equilibrium model. The best-fit temperature, kT=0.26, gave an unacceptably large reduced chi-squared of 2.8, and the model fit the data poorly below 0.5 keV and above 1 keV.

- We added a power law component to the model to try to fit the emission above 1 keV, and found a semi-acceptable value for chi-squared, 160 for 132 degrees of freedom.

- A second thermal component added to the model did not improve the fit significantly, yielding 158 for 130 degrees of freedom, and was not considered further.

- The comparison of the data to the best model is shown in the figure. The parameters of the best fit spectrum are:

Power law photon index	1.5 ± 0.17
Power law normalization (ph s^{-1} cm^{-2} sr^{-1} keV^{-1})	21. ± 1.5
MeKaL temperature (kT)	0.20 ± 0.02
MeKaL normalization (see below)	7.5 ± 2.2

5. DISCUSSION

- The thermal component normalization corresponds to an emission measure of $n_e^2 d = 0.0037$ $cm^{-6}pc$, which gives a surface brightness similar to that of our galaxy.

- The thermal component is ~ 20% of the unresolved emission from NGC 3184, and at a distance of 8.1 Mpc, the luminosity of the thermal component is ~ 2×10^{38} erg s^{-1}. We tentatively identify the thermal component with diffuse halo emission from NGC 3184.

- The luminosity of the power law component is ~ 10^{39} erg s^{-1}. We tentatively identify the power law component with emission from unresolved low mass X-ray binaries in NGC 3184.

6. CONCLUSIONS

- There appears to be halo emission from NGC 3184 located above the spiral arms of the galaxy with X-ray luminosity ~ 2×10^{38} ergs s^{-1}.

- Emission from another source, probably unresolved low mass X-ray binaries, has X-ray luminosity ~ 10^{39} ergs s^{-1}, roughly the same as that of the resolved point sources.

- We have not yet searched for spectral differences as a function of position on the face of the galaxy.

- Better tools for for working with extended diffuse emission would be helpful, especially tools for background determination.

A Chandra X-ray Observatory search for Local Bubble analogs in the near-face-on galaxy NGC3184

M. Juda (SAO),
W. T. Sanders, D. McCammon (Univ. of Wisconsin)
and W. Cui (Purdue U.)

Abstract

Various models for the evolution of Milky Way interstellar medium place the volume filling fraction of hot gas at values ranging from 10% to 90%. The opacity of the Galaxy to soft X-ray emission makes it difficult to constrain this fraction. X-ray Observations of near-by, face-on galaxies that are similar to the Milky Way should give us a better idea of the volume of the Galactic disk that is filled with hot gas. We present the results of a search for X-ray emission from regions analogous to the Local Bubble in the near-face-on galaxy NGC 3184 using data from the ACIS on the Chandra X-ray Observatory.

1 Introduction

The low energy diffuse X-ray background that we see in all directions provides evidence for a hot phase of the interstellar medium, with temperature near 10^6 K, that surrounds the solar system (McCammon & Sanders 1990, ARA&A 28, 657 and references therein; Snowden et al. 1995, ApJ 454, 643; Snowden et al. 1997, ApJ 485, 125), but the spatial distribution and filling factor in the Galactic disk are still unknown. Some theoretical models support isolated hot bubbles scattered throughout the disk, having a filling factor of order 10% with the Sun by chance inside one (Slavin 1989, ApJ 346, 718; Slavin & Cox 1992, ApJ 392, 131; Slavin & Cox 1993, ApJ 417,187). Other models have over 90% of the Galactic disk filled with hot plasma (McKee & Ostriker 1977, ApJ 218, 148) with the Sun located in a typical environment. An understanding of the role of the hot plasma in the evolution and behavior of the interstellar medium requires the resolution of this fundamental ignorance.

This million degree plasma is primarily observable in soft X-rays in the 0.1 keV–0.3 keV range, and we see in the soft X-rays not only the Local Bubble of hot plasma, but also several other bubbles within a few hundred parsecs, those in Sco-Cen, Monoceros-Gemini, and Orion-Eridanus. How pervasive is this hot ISM phase is not known, because the large cross-section for soft X-ray absorption by the neutral interstellar material prevents us from seeing beyond the nearest few hundred parsecs in the disk of our Galaxy. In the 0.5–1 keV range, where the characteristic temperature is several million degrees, the observed intensity is due to a mixture of extragalactic and galactic emission. Some of the galactic emission in the 0.5–1 keV band is from large diffuse features, such as the Sco-Cen bubble, the Orion-Eridanus bubble, and the Galactic bulge, but there appear to be components within both the Galactic disk and the Galactic halo that do not have well-understood origins.

Observations of nearby spiral galaxies provide an opportunity to study a wider area of the galactic disk than we can in the Galaxy. Upper limits were derived for the diffuse X-ray emission of M101 using *Einstein* IPC observations (McCammon & Sanders 1984, ApJ 287, 167). These limits were used by Cox & McCammon (1986, ApJ 304, 657) to constrain supernova rates and interstellar densities. Using *ROSAT* observations, Snowden & Pietsch (1995, ApJ 452, 627), found evidence for diffuse emission from M101, mostly in the 1/4 keV band, clearly visible over the inner 15 kpc radius. They concluded the emission was most likely from the halo of M101, and was at a level similar to the brightest 1/4 keV halo emission seen in our galaxy. *ROSAT* observations of other nearby spiral galaxies show that in addition to point sources associated with the galaxies, there is evidence for emission that is unresolved and covers a significant fraction of the face of the galaxy, presumably arising from a hot ISM (Ehle et al. 1995, A&A 295, 289; Snowden and Pietsch 1995, ApJ 452, 627; Cui et al. 1996, ApJ 468, 102; Read et al. 1997, MNRAS 286, 626).

The Chandra X-Ray Observatory (CXO), with its combination of high angular resolution, provides the capability to separate point sources from the diffuse emission and resolve bright bubbles of diffuse emission on size scales of 100 pc at a distance of 10 Mpc. In this poster, we present CXO ACIS data from two observations of the nearby (8 Mpc), near-face-on spiral galaxy NGC 3184, concentrating on a search for analogs to the bubbles within our galaxy. Table 1 lists the parameters of NGC 3184. A discussion of the diffuse emission is the subject of paper 32.24 at this conference.

2 Data

NGC 3184 was observed using the ACIS-S twice, on 2000-Jan-08 and on 2000-Feb-03 (ObsIDs 804 and 1520 respectively). The pointing direction was offset by 2.1 arcmin so that the galaxy was centered on the S3 (backside illuminated) CCD. Table 2 gives the parameters of the two observations. We used standard CIAO tools to incorporate gain and position corrections to the event lists and to filter and extract subsets of the data.

We started our search for galactic bubble analogs by using the CIAO tool *wavdetect* to search for sources over a range of scale sizes. For each observation, the field searched was a 1024×1024 pixel ($\sim 8.4 \times 8.4$ arcmin) region centered on NGC 3184. We selected events from the S3 CCD that have energies less than 5 keV and that do not occur on the node boundary. The analogs of the galactic bubbles should not have much emission at energies above 1 keV but by using a wider energy band we expect to find hard point sources that might contribute emission at lower energies. We conducted the search on scale sizes in the range 1–16 ACIS pixels (0.492 arcsec/pixel), incrementing the scale size in powers of $\sqrt{2}$. A total of 64 sources were detected in ObsID 804 and 47 sources were detected in ObsID 1520, 40 of the detections were in common between the two observations. Figure 1 shows the reconstructed images of the source detections of the two observations along with an image of NGC 3184 from the Digital Sky Survey. Variability in some of the sources between the two observations is apparent from a comparison of the two images. Tables 3 and 4 lists the source detections in the two observations; given for each detection is the R.A and Dec, the number of the source in the detection list, the net counts determined for the source, the significance level, the ratio of the observed size of the source to the expected size of the PSF and the source ID in the other observation.

We expect most of the diffuse galactic emission to have energies below 1 keV. We performed the same *wavdetect* source search on the fields restricting the energies to less than 1 keV and find fewer sources, partly due to reduced counts in the sources but also because of source spectra. In addition to the source identifications, we used *wavdetect* to generate reconstructed background images from the two observations; these background images are displayed in figure 2. These two background images do not agree in detail but in general, the brighter emission is coincident with the spiral arms. Among the reason for differences in the two images are incomplete removal of sources, variability in the unremoved sources, and the underlying counts statistics.

Improved images of the "background" below 1 keV can be made by removing the contribution from the detected sources. We removed events from the observations that lie within the union of the source regions from *wavdetect* for the sources in tables 3 and 4. The resulting images were then smoothed with a gaussian ($\sigma = 16$ pixels); these images are shown in figure 3.

3 Discussion

3.1 Sources

The bubbles that we see in the Galaxy have typical diameters of 100 pc; at the distance of NGC 3184, they would subtend an angle of $\sim$ 2.5 arcsec or about 5 pixels in ACIS. Over most of the field that we searched for sources the size of the PSF is expected to be ≤ 1 pixel and so we should have no problem resolving bubbles of this size. There is no significant evidence that any of the source detections have extent beyond that of a point source. Thus, our source detections provide no obvious bubble candidates.

3.1.1 SN 1999gi

There was a supernova reported in NGC 3184 (IAU Circular 7329) last December 9, SN 1999gi; the location given was RA=10:18:16.66 Dec=+41:26:28.2. The CXO observations of NGC 3184 were performed roughly one and two months after the discovery. A source was detected at the location of SN 1999gi in both of the observations: source ID 11 in ObsID 804 and source ID 4 in ObsID 1520. The observed rate for X-rays with energies less than 5 keV was $8.0 \pm 1.4 \times 10^{-4}$ counts s^{-1} in ObsID 804 and $6.5 \pm 1.6 \times 10^{-4}$ counts s^{-1} in ObsID 1520. No significant change in the rate is detected in the observations taken one month apart. About half of the rate comes from energies below 1 keV. There are not enough photons in the detections to determine a spectrum but using a mean energy per photon of 1 keV, the fluxes are $1.7 \pm 0.3 \times 10^{-15}$ ergs cm^{-2} s^{-1} and $1.4 \pm 0.3 \times 10^{-15}$ ergs cm^{-2} s^{-1}. At 8.0 Mpc, this flux implies a luminosity of 1.2×10^{37} ergs s^1.

3.2 Background Images

The failure to detect any galactic bubble analogs in the *wavdetect* search could be due to their surface brightness relative to the more diffuse emission and other background in the images. In ObsID 804, the sources were identified against a background of 0.025–0.035 counts per pixel, which translates to a surface-brightness of $\sim 1 \times 10^{-2}$ counts s^{-1} $arcmin^{-2}$. When the energy range is restricted to less than 1 keV, the surface-brightness of the background is only halved. Within the Galaxy, the Local Bubble and Sco-Cen bubble have *ROSAT* PSPC measured surface-brightnesses of $\sim 1 \times 10^{-3}$ counts s^{-1} $arcmin^{-2}$. A prediction of the ACIS-S rate we would expect to see from a bubble with this surface brightness depends strongly on the assumed spectrum. Assuming a collisional plasma with a temperature of $10^{6.3}$ K (typical of the Sco-Cen bubble) absorbed by a HI column density of 3×10^{20} cm^{-2}, we used PIMMS to derive an expected surface brightness of $\sim 1 \times 10^{-3}$ counts s^{-1} $arcmin^{-2}$. This bubble would be difficult to detect against the observed background surface-brightness.

The Sco-Cen bubble and the Local Bubble appear to be confined, i.e. they have not broken out into the Galactic halo. Larger hot bubbles, Super-bubbles, are a more likely to be a supply of hot gas for the Galactic halo. Since they are more energetic, we would expect the Super-bubbles to be more visible against the more diffuse emission. Figures 4 and 5 are comparisons of the backgrounds at energies below 1 keV, smoothed with a $\sigma = 8$ pixel gaussian and the Digital Sky Survey image for ObsIDs 804 and 1520 respectively. The contours levels that are plotted were chosen to select the peaks of the X-ray emission. Both observations show evidence for enhanced emission at the galactic center as well as for enhanced emission coincident with a bright optical feature south-west of the center.

Both of these regions of enhanced emission are several times brighter than the surrounding background. A peaking of the emission in the galactic center was observed in the *ROSAT* observation of NGC 3184 (Cui et al. 1996) and is typical of other observed spiral galaxies. The south-west enhancement, by its association with the bright optical feature is an obvious candidate for a Super-bubble. Within an 8-pixel radius region centered on this feature the average surface-brightness is 1.6×10^{-2} counts s^{-1} arcmin^{-2} above the the surrounding level or ~ 16 times brighter than our expectation from the Sco-Cen bubble.

4 Summary

Our search for analogs of Galactic bubbles in NGC 3184 did not reveal and definitive detections. Confined bubbles, such as the Local Bubble, may be too faint to see against the more diffuse emission from the galaxy, the bulk of which presumably comes from the galactic halo. Bubbles that have broken out of the disk and are contributing hot gas to the galactic halo are expected to be brighter. While we do not have a "smoking gun" for a Super-bubble detection, the association of bright peaks in the background maps with the galactic center and a region of enhanced optical emission are suggestive of blow-out regions supplying hot gas to the galactic halo.

Table 1: Properties of NGC 3184

R.A.	10:18:17.26
Dec	+41:25:25.9
Hubble Type	Sc
Distance (Mpc)	8.0
Size (arcmin)	7.4/6.9
Galactic NH (cm^{-2})	1.15×10^{20}

Table 2: CXO ACIS Observations of NGC 3184

ObsID	804	1520
Aim-point R.A.	10:18:14.116	10:18:06.956
Aim-point Dec	+41:27:44.17	+41:27:02.19
Spacecraft Roll (degrees)	101.993097	142.591636
Observation Start	2000-01-08T00:51:42	2000-02-03T10:42:17
Exposure Time (s)	42310.40	26524.44

Table 3: ObsID 804 *wavdetect* sources

R.A.	Dec	Source ID	Net Counts	Significance	PSF Ratio	ObsID 1520 ID
154.47974	41.45268	46	30.4 ± 5.7	12.1	1.10	
154.48227	41.43542	45	13.2 ± 3.7	5.9	0.77	32
154.49341	41.36440	58	34.1 ± 6.2	10.8	0.84	
154.49428	41.43419	31	64.3 ± 8.1	25.1	1.10	9
154.49823	41.40443	54	22.4 ± 5.0	7.9	1.15	
154.50979	41.39764	30	138.9 ± 12.0	40.8	1.22	18
154.51317	41.45342	29	19.0 ± 4.5	8.2	1.28	30
154.51346	41.42568	44	5.7 ± 2.4	2.8	0.71	
154.51383	41.46067	53	5.6 ± 2.4	2.7	0.63	
154.51873	41.42900	28	28.8 ± 5.5	12.1	1.16	
154.52742	41.43499	27	13.3 ± 3.7	6.1	0.99	39
154.52862	41.43753	18	7.6 ± 2.8	3.7	0.49	29
154.52882	41.37300	61	13.5 ± 4.4	3.9	1.35	
154.52897	41.40619	26	66.5 ± 8.3	23.7	1.22	8
154.53014	41.42571	52	5.5 ± 2.4	2.6	0.81	
154.53195	41.47429	25	15.3 ± 4.0	7.0	1.39	47
154.53270	41.44368	43	3.7 ± 2.0	1.8	0.60	
154.53461	41.39224	42	43.7 ± 6.9	14.4	1.11	28
154.53733	41.38464	41	32.3 ± 6.0	10.4	1.14	42
154.53821	41.35836	63	4.5 ± 2.4	1.8	0.54	46
154.53935	41.43351	17	10.6 ± 3.3	5.1	0.62	
154.53994	41.39466	40	9.2 ± 3.2	4.1	0.52	
154.54504	41.42774	16	27.0 ± 5.3	11.7	1.02	26
154.54886	41.44177	39	7.5 ± 2.8	3.5	1.21	

R.A.	Dec	Source ID	Net Counts	Significance	PSF Ratio	ObsID 1520 ID
154.55040	41.40583	15	423.8 ± 20.7	123.2	1.13	7
154.55167	41.45156	14	51.9 ± 7.3	22.1	1.60	6
154.55668	41.38651	51	40.6 ± 6.8	11.6	1.32	41
154.55716	41.42411	24	20.0 ± 4.6	8.6	1.29	17
154.55719	41.46496	23	6.6 ± 2.6	3.2	1.06	
154.55828	41.41060	38	6.4 ± 2.6	3.0	0.69	
154.55912	41.36708	64	4.6 ± 2.4	1.9	0.45	
154.56034	41.37403	60	5.1 ± 2.4	2.2	0.49	37
154.56206	41.44420	13	10.6 ± 3.3	5.0	1.04	
154.56235	41.43538	12	47.8 ± 7.0	20.0	1.29	5
154.56822	41.35941	57	11.0 ± 3.7	3.8	0.72	45
154.56935	41.44122	11	33.9 ± 5.9	14.3	1.32	4
154.56999	41.42941	10	17.1 ± 4.2	7.5	1.03	36
154.57014	41.42582	22	9.2 ± 3.2	4.1	0.96	16
154.57037	41.42392	9	90.6 ± 9.6	32.5	1.45	15
154.57081	41.42449	37	33.6 ± 5.9	13.6	1.29	
154.57604	41.37256	56	15.6 ± 4.6	4.5	1.23	
154.57855	41.43225	8	86.5 ± 9.4	34.7	1.39	3
154.57954	41.44512	21	5.6 ± 2.4	2.7	0.90	24
154.57957	41.42489	55	7.2 ± 2.8	3.3	1.05	
154.58177	41.43766	7	23.3 ± 4.9	10.6	1.02	14
154.58199	41.44576	6	17.3 ± 4.2	7.9	0.94	2
154.59039	41.44091	20	12.1 ± 3.6	5.3	1.40	35
154.59070	41.43602	5	94.8 ± 9.8	39.2	1.18	13
154.59583	41.48956	4	120.7 ± 11.0	49.8	1.32	12
154.59591	41.46172	3	506.9 ± 22.6	171.1	1.53	1
154.59633	41.42021	2	93.2 ± 9.7	36.0	1.07	11
154.59823	41.43843	1	60.6 ± 7.9	24.6	1.25	10
154.59885	41.38251	50	37.1 ± 6.3	12.7	0.93	21
154.59940	41.41487	36	26.1 ± 5.3	9.9	1.10	20
154.59966	41.35737	49	88.5 ± 9.9	20.3	1.38	40
154.60226	41.41943	35	8.5 ± 3.0	4.0	0.58	19
154.61138	41.41726	19	47.3 ± 7.1	16.5	1.31	
154.62672	41.45145	34	7.6 ± 2.8	3.7	0.59	
154.62734	41.45166	33	6.6 ± 2.6	3.2	0.68	
154.62945	41.44518	32	9.5 ± 3.2	4.5	0.63	34
154.63028	41.41382	48	26.6 ± 5.4	9.5	1.00	44
154.63920	41.40642	47	53.6 ± 7.6	16.4	1.23	33
154.66012	41.36639	62	11.1 ± 3.7	3.8	0.73	
154.66305	41.39631	59	10.9 ± 3.7	3.7	0.78	

Table 4: ObsID 1520 *wavdetect* sources

R.A.	Dec	Source ID	Net Counts	Significance	PSF Ratio	ObsID 1520 ID
154.48234	41.43560	32	7.7 ± 2.8	3.7	0.78	45
154.48761	41.38560	31	8.3 ± 3.0	3.8	0.68	
154.49425	41.43427	9	35.4 ± 6.0	16.4	1.27	31
154.50977	41.39762	18	36.4 ± 6.1	16.7	0.83	30
154.50993	41.47323	43	1.9 ± 1.4	1.0	0.00	
154.51317	41.45351	30	7.6 ± 2.8	3.7	1.64	29
154.52733	41.43491	39	4.8 ± 2.2	2.4	1.17	27
154.52879	41.43752	29	6.7 ± 2.6	3.3	1.46	18
154.52893	41.40623	8	47.1 ± 6.9	20.5	1.11	26
154.53194	41.47438	47	6.7 ± 2.6	3.4	1.02	25
154.53437	41.39222	28	12.3 ± 3.6	5.6	0.85	42
154.53727	41.38439	42	4.7 ± 2.2	2.3	0.48	41
154.53770	41.41464	38	2.7 ± 1.7	1.4	0.53	
154.53809	41.42248	27	8.5 ± 3.0	4.1	1.07	
154.53876	41.35818	46	8.5 ± 3.2	3.4	0.81	63
154.54480	41.42773	26	11.4 ± 3.5	5.3	1.75	16
154.55033	41.40587	7	237.7 ± 15.5	86.7	1.21	15
154.55170	41.45158	6	33.4 ± 5.8	15.3	1.60	14
154.55663	41.38641	41	7.3 ± 2.8	3.4	0.63	51
154.55721	41.42413	17	13.5 ± 3.7	6.4	1.12	24
154.56038	41.37444	37	9.1 ± 3.2	4.0	0.64	60
154.56230	41.43534	5	25.3 ± 5.1	11.4	1.22	12
154.56884	41.35940	45	13.8 ± 4.1	4.6	1.17	57
154.56936	41.44121	4	17.3 ± 4.2	7.9	1.14	11
154.56993	41.42935	36	6.6 ± 2.6	3.2	0.86	10
154.57017	41.42586	16	6.6 ± 2.6	3.2	0.67	22
154.57037	41.42395	15	51.4 ± 7.3	20.4	1.41	9
154.57630	41.44374	25	5.7 ± 2.4	2.8	0.54	
154.57857	41.43225	3	91.8 ± 9.6	38.6	1.20	8
154.57968	41.44518	24	10.5 ± 3.3	5.0	1.10	21
154.58179	41.43760	14	6.7 ± 2.6	3.3	0.69	7
154.58197	41.44580	2	32.5 ± 5.7	15.2	1.00	6
154.58884	41.43809	23	5.7 ± 2.4	2.9	0.00	
154.59050	41.44105	35	9.5 ± 3.2	4.4	1.13	20
154.59093	41.43604	13	45.2 ± 6.8	20.1	1.02	5
154.59434	41.47285	22	4.8 ± 2.2	2.4	0.71	
154.59567	41.46159	1	79.4 ± 8.9	36.9	0.76	3
154.59567	41.48945	12	45.2 ± 6.8	20.0	0.96	4
154.59635	41.42020	11	56.3 ± 7.6	21.9	1.23	2
154.59805	41.43836	10	35.3 ± 6.0	16.0	1.01	1
154.59872	41.35704	40	33.4 ± 6.2	10.1	0.97	49
154.59924	41.38224	21	43.8 ± 6.9	13.5	1.24	50
154.59929	41.41491	20	10.6 ± 3.3	5.2	0.61	36
154.60206	41.41957	19	6.5 ± 2.6	3.1	0.59	35
154.62961	41.44502	34	16.8 ± 4.4	6.2	1.03	32
154.63138	41.41447	44	6.8 ± 2.8	2.8	0.72	48
154.63892	41.40628	33	23.8 ± 5.3	7.4	1.18	47

Figure 1: Reconstructed images of *wavdetect* sources from the two observations. Sources are displayed with a logarithmic intensity scale. Also shown is the Digital Sky Survey image of NGC 3184. The large circle in each panel corresponds to a diameter of 7.14 arcmin.

Figure 2: Reconstructed images of the "background" below 1 keV in two observations along with the Digital Sky Survey image. False color indicates surface brightness with violet and blue at the faint end and red and white at the bright end.

Figure 3: Images of the "background" below 1 keV in two observations along with the Digital Sky Survey image. The X-ray images were generated by a gaussian smoothing ($\sigma = 16$ pixels) of images where the events from the source regions identified by *wavdetect* using energies less than 5 keV have been removed. False color indicates surface brightness with violet and blue at the faint end and red and white at the bright end.

Figure 4: Background at energies below 1 keV for ObsID 804 smoothed with a $\sigma = 8$ gaussian and the Digital Sky Survey image. The contours plotted in both panels are identical and are selected to indicate the peaks of the X-ray emission.

Figure 5: Background at energies below 1 keV for ObsID 1520 smoothed with a $\sigma = 8$ gaussian and the Digital Sky Survey image. The contours plotted in both panels are identical and are selected to indicate the peaks of the X-ray emission.

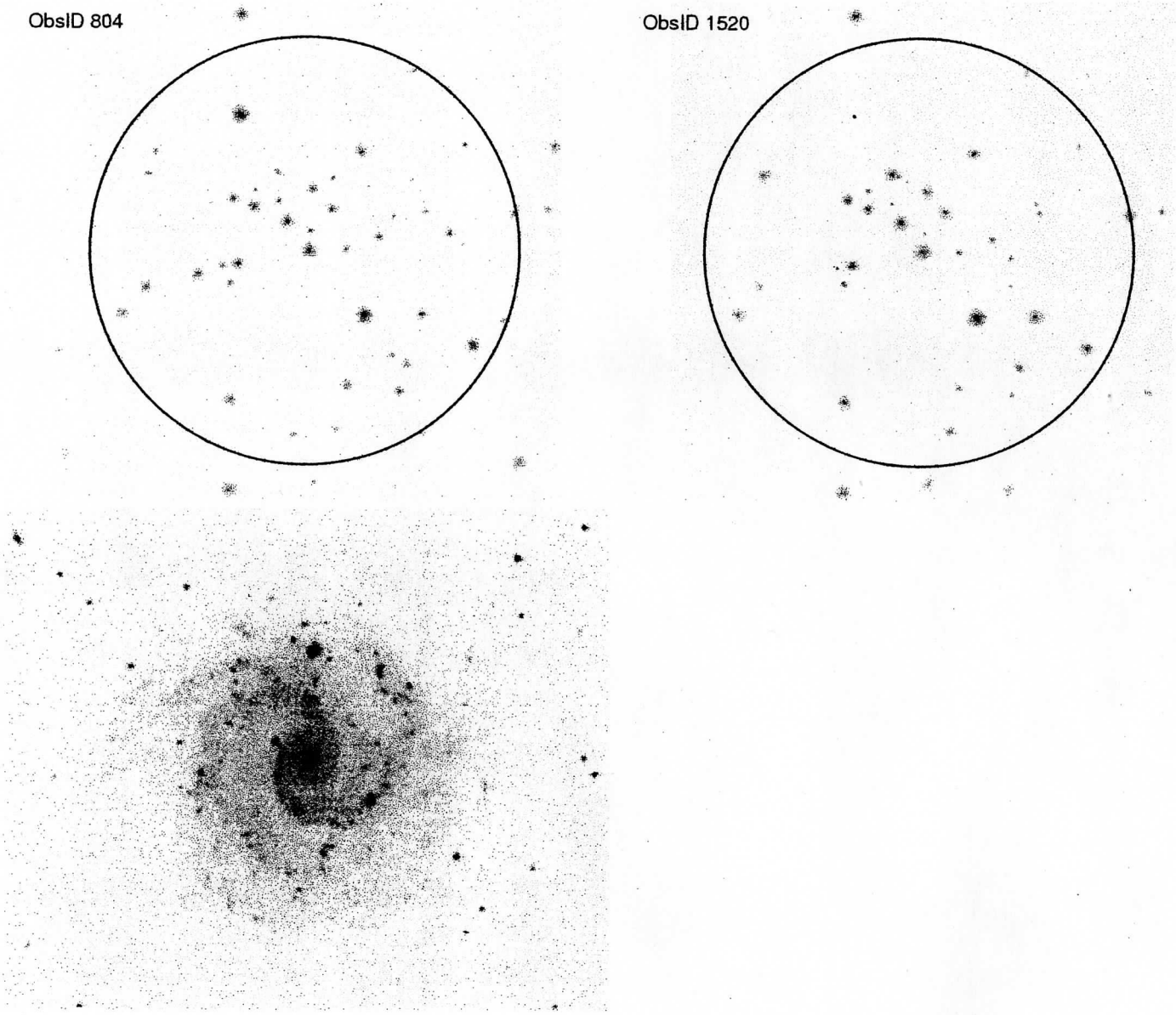

FIG 1

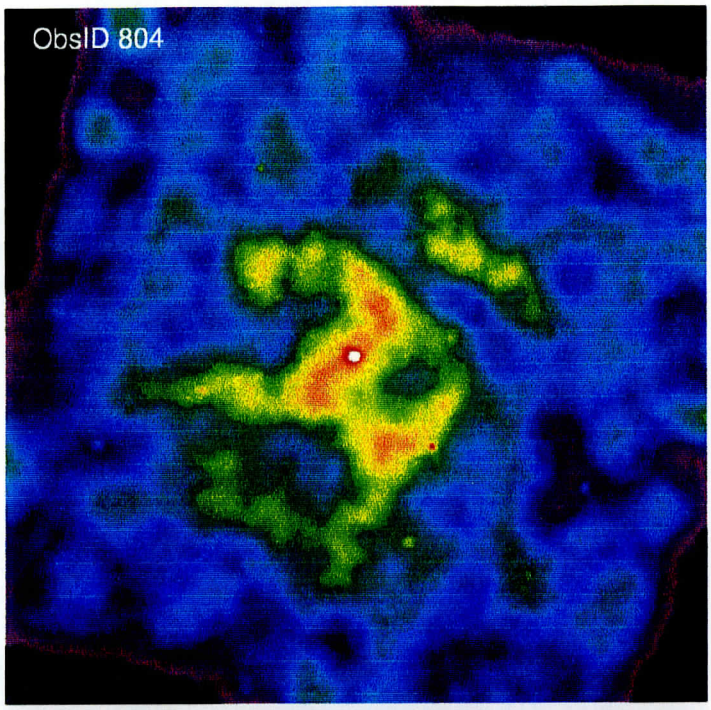

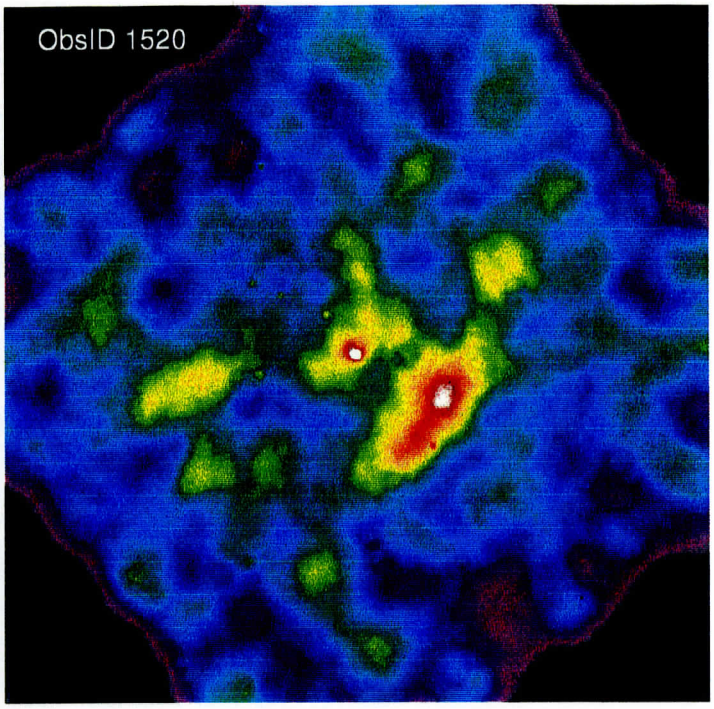

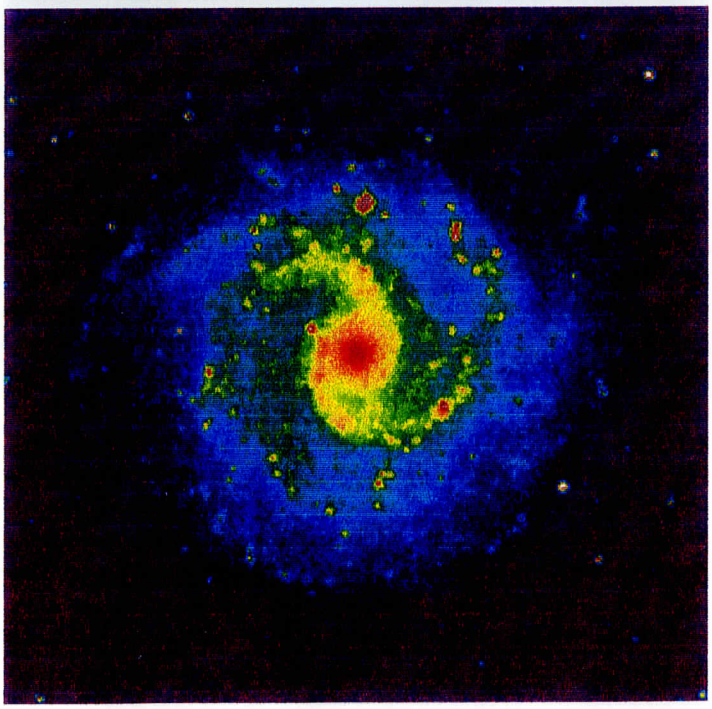

FIG. 2

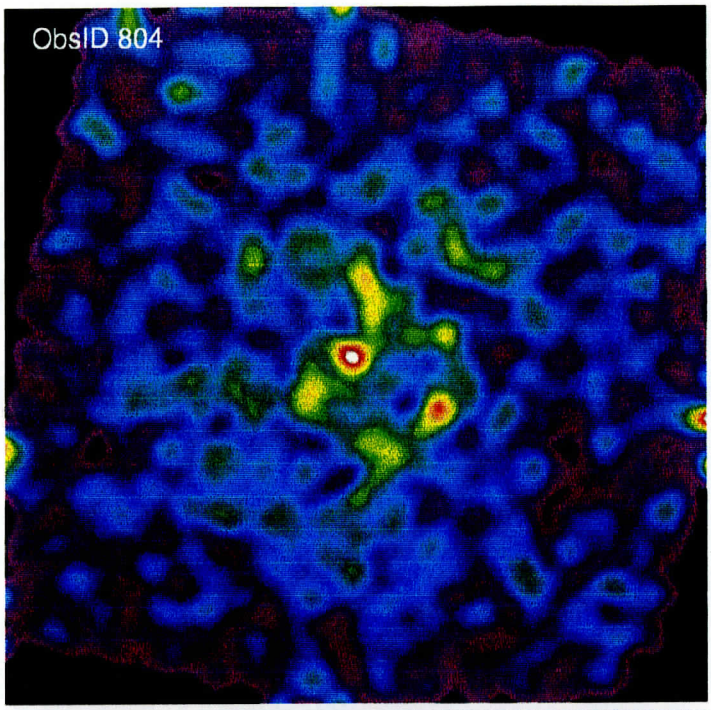

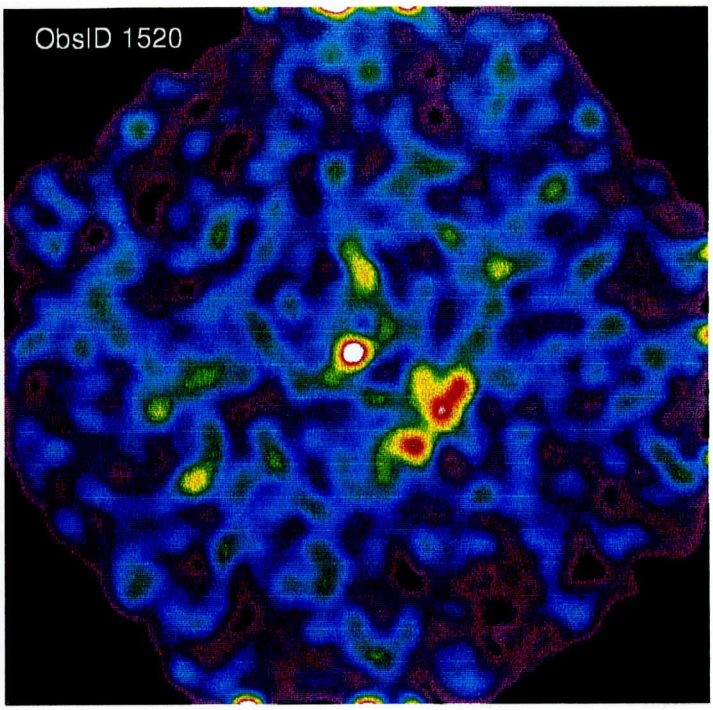

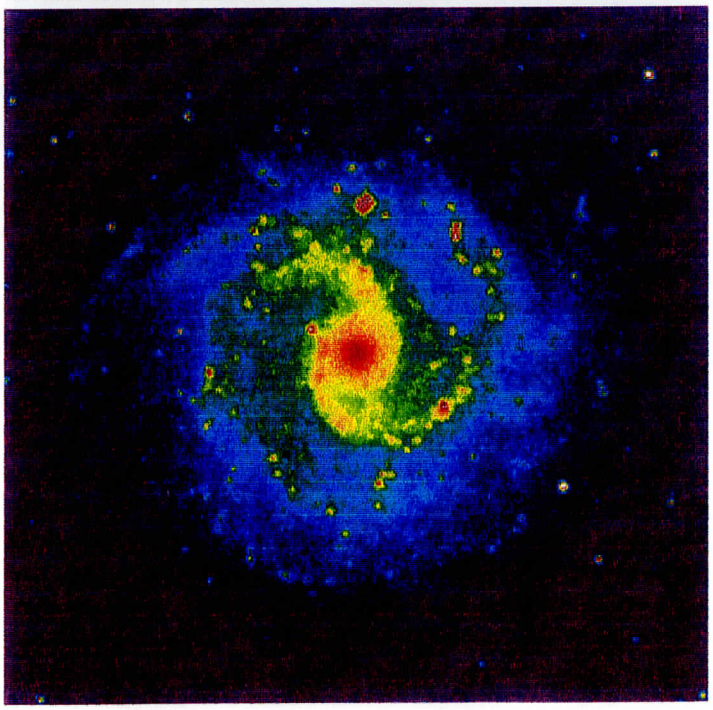

FIG. 3

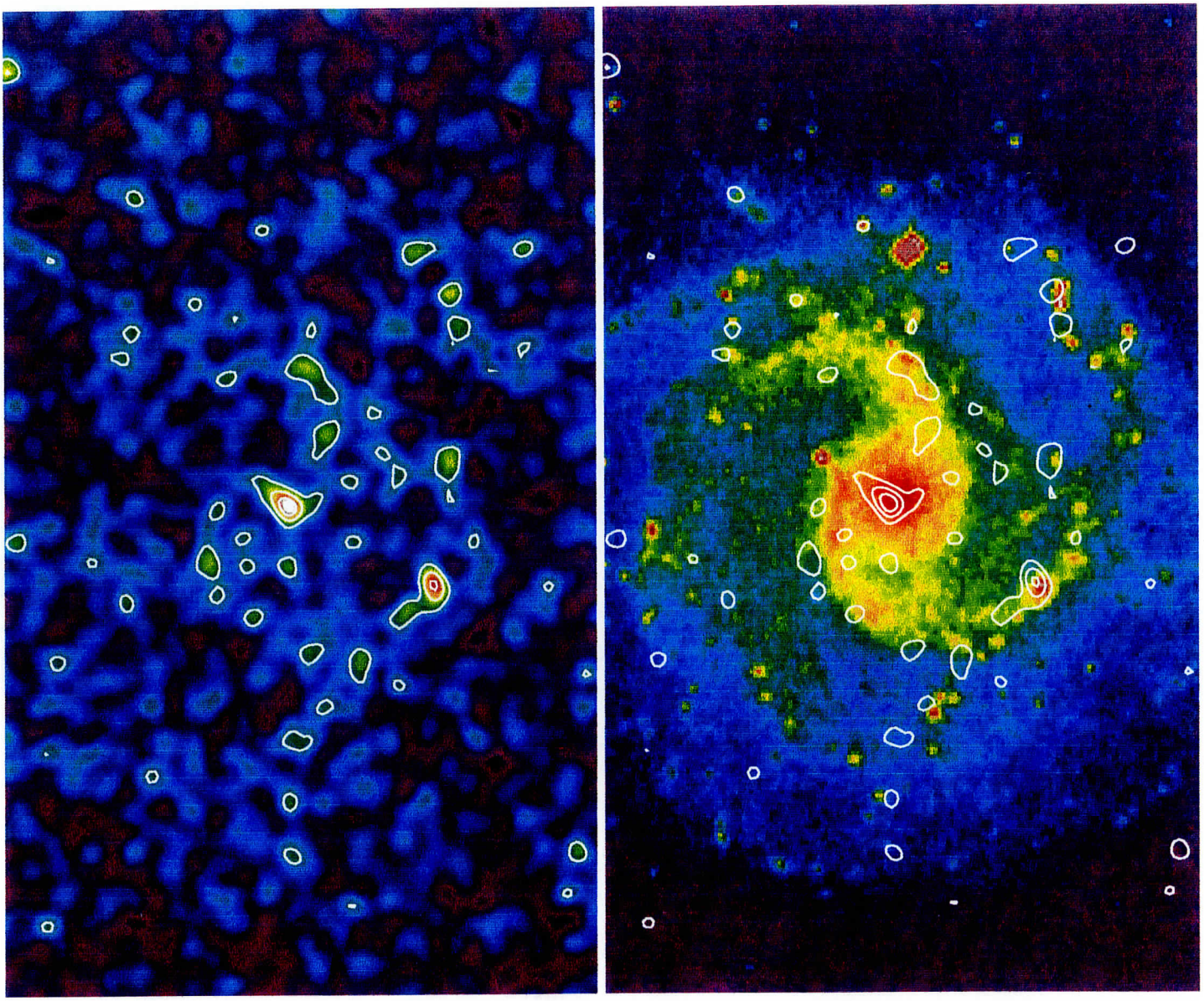

FIG. 4

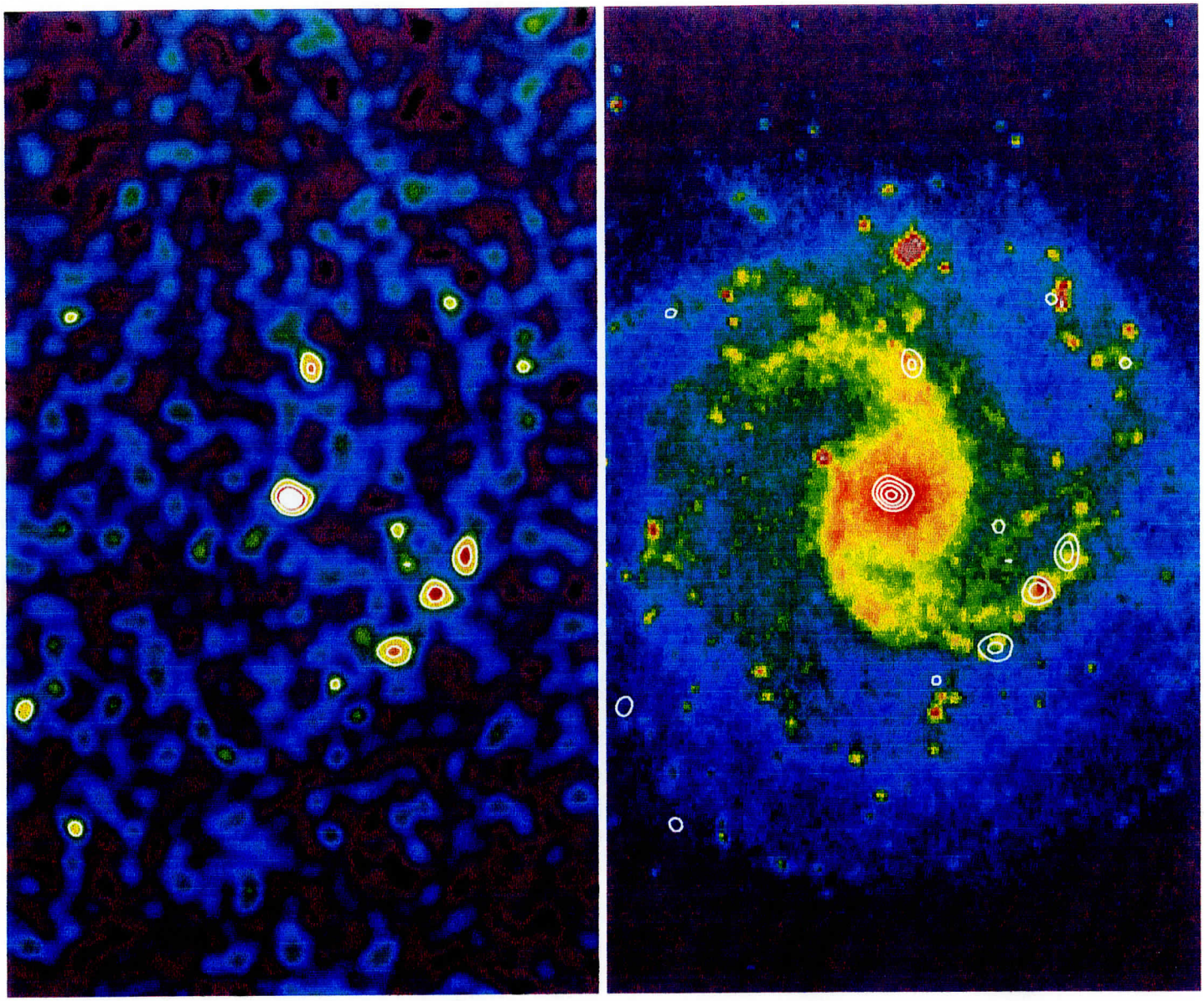

FIG. 5